The correlation between mass-averaged SAR and temperature elevation in human head model exposed to RF near-fields from 1 to 6 GHz

Akimasa Hirata and Osamu Fujiwara

Nagoya Institute of Technology, Japan
Corresponding author: Dr. Akimasa Hirata
ahirata@nitech.ac.jp

Abstract

In the present study, we investigate the relationship between the mass-averaged specific absorption rate (SAR) and temperature elevation in anatomically based Japanese head models due to the dipole antenna. A homogeneous cubical model is also used as a basis for the investigation. The frequency region considered is from 1 to 6 GHz. Our attention is focused on the averaging mass of SAR, which maximizes the correlation with local temperature elevation. An averaged SAR over 10 g was found to reasonably correlate with local temperature elevation even for frequencies from 3 to 6 GHz. The dominant factor influencing the correlation between mass-averaged SAR and temperature elevation is suggested to be the thermal diffusion length in biological tissue, together with the penetration depth of radio-frequency waves. The correlation of local temperature elevation to mass-averaged SAR is largely influenced by the blood perfusion rate, while at most 10% or less is due to the pinna, model inhomogeneity and the antenna position relative to the head model.

Keywords: specific absorption rate (SAR), SAR averaging mass, temperature elevation, correlation, guidelines/standards

1. Introduction

In recent years, there has been increasing public concern about adverse health effects due to electromagnetic fields. Therefore, international standardization bodies have been regulating safety guidelines/standards for human protection from electromagnetic fields (e.g., ICNIRP 1998; IEEE 2005). Peak mass-averaged SAR (specific absorption rate) is used as a metric for radio-frequency (RF) localized exposures. Even though peak mass-averaged SAR is used as a metric for human protection, physiological effects and damage to humans due to RF energy could be induced by the temperature elevation. A temperature elevation of 4.5^{o}C in the brain has been noted to be an allowable limit, which does not lead to any physiological damage for exposures of more than 30 minutes (Guyton and Hall 1952). It has also been reported that a temperature elevation in the rabbit hypothalamus of 0.2–0.3 ◦C leads to altered thermoregulatory behavior (Adair et al 1984). The threshold temperature of the pricking pain in the skin is 45^{o}C, corresponding to the temperature elevation of 10-15^{o}C (Hardy *et al*. 1952).

There are/were several differences for the metric in different guidelines/standards, although their scientific rationales should be identical. A recent notable trend in international guidelines/standards is that an averaging mass for SAR has been harmonizing to 10 g since that prescribed in the IEEE standard (2005) has been changed from 1 g to 10 g. One of the rationales for the revision in the IEEE standard (2005) is the correlation between mass averaged-SAR and temperature elevation in the brain (Bernardi et al. 2000, Gandhi et al. 2001, Hirata et al. 2003a, Hirata and Shiozawa 2003b, Ibrahiem et al. 2005, Van Leeuwen et al. 1999, Wang and Fujiwara 1999) and the eye (Hirata et al. 2000, Hirata 2005), which has been computed with anatomically-based head models. The applicable upper frequency of peak spatial-average SAR is 3 GHz in the IEEE standard (2005) and 10 GHz in the ICNIRP guidelines (1998). In the standard for SAR measurement, the upper frequency is 3 GHz for the wireless devices used in close proximity of the head in IEEE standard (2003) and IEC standard (2005) and 6 GHz for body-mounted devices in the draft standard of IEC (2008). In these circumstances, much attention has been paid to the effective frequency region where a 10 g-averaged SAR is appropriate as a metric for estimating local temperature elevation. After the IEEE standard (2005) was published, this kind of work was still being reported by different groups with high-resolution numeric human phantoms (e.g., Buccella et al. 2007, Flyckt et al. 2007, Hirata et al. 2007, Laakso 2009).

As summarized in the IEEE standard (2005), most previous studies have paid attention to the correlation between *peak* mass-averaged SAR and *peak* temperature elevation only. In order to obtain insight on the SAR averaging mass, the mass-averaged SAR and the temperature

elevation over the head/body model has been recently investigated. Bit-Babik et al. (2007) investigated the effect of mass for spatial-average SAR on the correlation with temperature elevation for exposure to a plane wave in the frequency between 30 MHz and 1 GHz. From the aspect of the correlation with temperature elevation, a SAR average mass of 5-10 g was found to be reasonable over a wide frequency band. Razmadze et al. (2009) investigated the effect of the SAR averaging scheme and mass on the correlation with temperature elevation for a plane wave exposure in the frequency between 30 MHz and 800 MHz. From the aspect of the correlation with temperature elevation, an averaging mass of 10 g was shown to be more appropriate than 1 g over wide frequencies. However, the far-field source or plane wave was considered in these studies, although spatial-average SAR is a metric to protect humans from near-field exposures (ICNIPR 1998, IEEE 2005). Hirata et al. (2008) investigated that the correlation between mass-averaged SAR and temperature elevation over the head due to a dipole antenna from 800 MHz to 3 GHz (Hirata et al. 2008). Then, a SAR averaging mass of 10−30 g is shown to be a good metric to correlate local temperature for the above frequencies.

In the present study, we investigate the effect of SAR averaging mass on the correlation with temperature elevation in the head due to a dipole antenna in order to clarify the rationale of SAR averaging mass and its applicable frequency region. The frequencies considered were from 1 to 6 GHz. The correlation between mass-averaged SAR and temperature elevation was investigated statistically for all the voxels of the head model. In order to investigate the effect of frequency and thermal constants on mass-averaged SAR and temperature elevation, a homogeneous cubical model with its side length similar to that of the human head is used first. Then, anatomically based head models are used to confirm the finding for the homogeneous cubical model.

2. Model and Methods

A. Head Models

For fundamental discussion, we used a homogeneous cubical model comprised of 2/3 muscle as shown in Fig. 1. The height and width of the cubical model are both 200 mm, which is similar to those of human heads. Its depth is shortened to 100 mm since the penetration depth is at most several centimeters even at 1 GHz, which is the lowest frequency considered.

Anatomically based head models developed at the Nagoya Institute of Technology (NIT) (Wang and Fujiwara 2002) and the National Institute of Information and Communications Technology (NICT) (Nagaoka et al. 2004) were used in the present study. The former head model is comprised of 17 tissues, including bone (skull), muscle, skin, fat, white matter, grey matter, cerebellum, and blood. The latter model is comprised of 51 tissues, allowing for the whole human body. Thus, only the head and neck parts were used for the present study. The

resolution of these models is 2 mm, and thus each cell is further divided into eight cells with a resolution of 1 mm in order to keep the computational accuracy as high as possible. An in-house smoothing algorithm with manual editing has been applied to maintain the reliability of the model. The width, depth, and height of the former anatomic model are 202 mm, 210 mm, and 228 mm, respectively, while 198 mm, 212 mm, and 260 mm are the latter model dimensions.

According to Laakso (2009), a cell resolution of 1 mm has been shown to be required for analysis at a frequency of 5 GHz. Even though we consider the frequency of 6 GHz, the simplified model is comprised of 2/3 muscle, the dielectric constant of which is smaller than the high water content tissues of actual humans. In addition, our attention here is on the correlation between mass-averaged SAR and local temperature. Thus, for both simplified shaped models and anatomically-based models, the correlation of SAR and temperature elevation was marginally influenced, when comparing the results using the models with the resolutions of 0.5 mm and 1 mm, although the data are not shown here to avoid repetition.

B. RF Dosimetry

The finite-difference time-domain method is used for conducting RF dosimetry in the human due to a dipole antenna. The side length of the cell is 1 mm, which matches the resolution of the head model. The electrical constants of the tissues are determined with a 4-Cole-Cole extrapolation (Gabriel 1996). For geometries in which wave-object interaction proceeds in the open region, the computational space has to be truncated by absorbing boundaries. In this study, a 12-layered PML was used. For calculating mass-averaged SAR, an algorithm specified in the IEEE C95.3 standard (2002) is used. Note that the cells in the pinna are not considered in the computation, as the pinna is treated as extremities in the standard.

C. Thermal Dosimetry

The temperature of the human body is calculated numerically with the finite-difference method by solving a well-known bioheat equation (Pennes 1948). The bioheat equation, which takes into account various heat exchange mechanisms such as heat conduction, blood perfusion, and EM heating, is represented by the following equation:

$$C(\mathbf{r})\rho(\mathbf{r})\frac{\partial T(\mathbf{r},t)}{\partial t} = \nabla\cdot(K(\mathbf{r})\nabla T(\mathbf{r},t)) + \rho(\mathbf{r})SAR(\mathbf{r}) + Q(\mathbf{r},t) - B(\mathbf{r},t)(T(\mathbf{r},t) - T_B(\mathbf{r},t)) \quad (1)$$

where T is the temperature of the tissue, T_b the blood temperature, K the thermal conductivity of the tissue, C the specific heat of the tissue, Q the metabolic heat generation, and B the term associated with blood perfusion.

The temperature elevation due to handset antennas can be considered as sufficiently small as to not to activate the thermoregulatory response. This response is neglected in our study.

Additionally, the blood temperature is assumed to be spatiotemporally constant, since the power absorption due to antennas (less than 1 W) is much smaller than the metabolic heat generation of a male adult (~100 W), resulting in a marginal body-core temperature elevation. Then, the blood temperature in (2) is simplified as constant ($T_B(\mathbf{r},t)$=37^{o}C). The boundary condition for (1) is given by

$$-K(r)\frac{\partial T(\mathbf{r},t)}{\partial n} = H \cdot (T_s(\mathbf{r},t) - T_e(t)) \tag{2}$$

where H, T_s, and T_e denote, respectively, the heat transfer coefficient, the surface temperature of the tissue, and the temperature of the air.

The thermal parameters used in the present study are the same as in Hirata et al. (2003a). They are mainly borrowed from Duck (1990). In addition to human tissue, we consider a cubical model comprised of 2/3 muscle. The mass density of 2/3 muscle is chosen as 1,000 kg/m^3. The heat transfer coefficient between the model surface and air was set to 5 W/m^2/^{o}C, which is the typical value at the room temperature of 23^{o}C (Fiala et al. 1999). Samaras et al. (2006) pointed out the weakness of the boundary condition for the bioheat equation when applied to the human model with the stair-casing approximation. Recently, an improved algorithm for reducing computational error has been proposed by Neufeld et al. (2007). Such an algorithm would be essential when calculating the temperature itself. However, that error marginally influences temperature *elevation*, as shown in Wang and Fujiwara (1999). Thus, we used the conventional formula given in this section.

D. Statistical Approach to Correlate Peak Mass-Averaged SAR and Temperature Elevation

We considered the relationship between mass-averaged SAR and temperature elevation at the datum point of the SAR averaging (IEEE 2002). The effect of SAR averaging mass on the correlation between mass-averaged SAR and temperature elevation was evaluated by the method of least square, assuming that the relation between temperature elevation (ΔT) and spatial-average SAR (SAR_{avg}) is linear;

$$\Delta T = a \cdot SAR_{avg}$$

where a or the ratio of $\Delta T/SAR_{avg}$ is called the ‘heating factor’ in the following discussion. This assumption could be reasonable since steady-state temperature elevation depends linearly on RF power absorption. The intercept in the equation is chosen as nonexistent as no temperature elevates without RF exposure. The coefficient of determination was used to evaluate the correlation. The less the calculated values depart from the regression line, the closer to unity the coefficient of determination is. Note that the heating factor is meaningful only for sufficiently large coefficient of determination. The SAR around the center of the head and the opposite side from the antenna is extremely small for the frequencies considered here since the

electromagnetic wave penetrates at most a few centimeters due to the small penetration depth (Gandhi et al. 1996, Watanabe et al. 1996).

Even though we pay attention to all the voxel in the human head model, voxels whose SAR is larger than the peak value multiplied by one hundredth are considered for computing the correlation. This is because computational accuracy may not be reliable for a small SAR value. Additionally, a small temperature elevation is not essential for human protection against EM wave exposure. Thorough discussion, including the scattered plots for mass-averaged SAR and temperature elevation, can be found in Hirata et al. (2008). It should be noted that the heating factor is shown to be marginally influenced by different antenna; e.g., monopole antenna and helical antenna) (Hirata and Shiozawa 2003).

E. Source and Exposure Scenario

The frequencies considered are 1.0 GHz, 1.5 GHz, 2 GHz, 2.5 GHz, 3 GHz, 4 GHz, and 6 GHz. The diameter of the dipole antenna is 0.5 mm. The lengths of the antenna are 143 mm, 93 mm, 69 mm, 55 mm, 45 mm, 33 mm, and 23 mm for 1.0 GHz, 1.5 GHz, 2 GHz, 2.5 GHz, 3 GHz, 4 GHz, and 6 GHz, respectively. The position of the antenna relative to the head model is given in Fig. 1. The feeding point is located on the horizontal plane where the center of the ear canal exists. The separation between the feeding point and the edge of the right pinna is 12 mm. The separation between the antenna and PML is put at 30 mm.

3. Computational Results

A. Effect of Frequency on Correlation between SAR and Temperature

We calculated the temperature elevation and mass-averaged SAR in the cubical model at frequencies from 1 to 6 GHz. The thermal conductivity K and the term related to blood perfusion rate B of the tissues are selected as 0.4 J/(s·^{o}C) and 5000 J/(s·^{o}C·m^{3}), respectively. These values are approximately the mean values of the skin and skull to which the dipole antenna is adjacent. Since we considered the temperature elevation at a thermally steady state, the heat capacitance does not influence the computational results.

We show in Fig. 2 the heating factor and the coefficient of determination for different frequencies from 1 to 6 GHz. As seen from Fig. 2 (a), the heating factor becomes larger with the averaging mass. The slopes of the curves become steeper with the higher frequency. These phenomena could be caused by the difference of skin depth; 20 mm at 1 GHz and 4 mm at 6 GHz for 2/3 muscle. Then, the mass-averaged SAR becomes smaller with the increase of SAR averaging mass as including the region where the SAR value is relatively small. The point to be stressed here is that all the lines come close to one another around 8-25 g. In other words, the heating factor marginally depends on the frequency for the SAR averaging mass specified above.

As seen from Fig. 2 (b), the coefficient of regression line peaks around 25 g at the frequencies of 1 and 2 GHz and around 10 g at 6 GHz.

B. Effect of Thermal Constants on Correlation between SAR and Temperature

As shown in Hirata et al. (2006), the dominant thermal constant influencing the temperature elevation in the biological tissues is the term associated with blood perfusion *B*. In this subsection, we investigate the effect of the blood perfusion rate on the correlation between the mass-averaged SAR and temperature elevation. We chose frequencies of 1 and 6 GHz, which are the lowest and highest frequencies considered in the present study. The blood perfusion rate has been changed from 2,500 J/(s·^{o}C·m^{3}) to 20,000 J/(s·^{o}C·m^{3}) which mostly covers that in the biological tissue (Duck 1990). As shown in Fig. 3 (a), the heating factor at 1 GHz varies by a factor of 5 to 7 even for the same mass-averaged SAR at the frequency of 1 GHz. As shown in Fig. 3 (c), a similar tendency was observed at 6 GHz. However, the slope of the curves becomes steeper at a higher frequency, similar to the case of Fig. 2 (a). From Fig. 3 (b), the SAR averaging mass which provides the maximal coefficient of determination at 1 GHz is 6 g for a blood perfusion rate of 20,000 J/(s·^{o}C·m^{3}) and 30 g for 1,000 J/(s·^{o}C·m^{3}). Similarly, from fig. 3 (d), it is 3 g for a blood perfusion rate of 20,000 J/(s·^{o}C·m^{3}) and 15 g for 1,000 J/(s·^{o}C·m^{3}).

C. Computational Results for Japanese Adult Male Model

This subsection presents the dependence of the heating factor and the coefficient of determination on the SAR averaging mass in the anatomically based head model. Figure 4 shows the heating factor and the coefficient of determination for the model developed at NIT. As seen from Fig. 4(a), the curves of heating factors at different frequencies cross one another at the SAR averaging mass of 10-20 g. This averaging mass coincides reasonably with the results for the cubical model. For the corresponding averaging mass, the difference in the heating factor is less than 20% at the same frequency and the coefficient of determination is mostly above 0.75. The coefficient of determination peaks at 6 g at 6 GHz and 10 g at 1 GHz.

Figure 5 shows the heating factor and the coefficient of determination for the model developed at NICT. Similar to the case in Fig. 4 (a), the curves of heating factors at different frequencies cross one another at the averaging mass of 10-30 g. The heating factors for the NICT model is 15-20% larger than those for the NIT model at each frequency. The coefficient of determination peaks at 10 g at 6 GHz while 20 g at 1 GHz. From Fig. 4 (b) and Fig. 5 (b), the coefficient of determination becomes somewhat smaller at 4 and 6 GHz. Then, the coefficient of determination at these frequencies is 10-15% smaller than those smaller than 3 GHz. However, the coefficients were still larger than 0.7.

D. Effects of Model Heterogeneity, Pinna and Antenna Position on the Correlation

This subsection first discusses the effect of *i*) model heterogeneity and *ii*) pinna on the SAR averaging mass in the anatomically based head model developed at NIT. The effect of pinna on the SAR distribution has been extensively discussed in Gandhi et al. (1996), Watanabe et al. (1996) and Burkhart and Kuster (2000). For comparison, the realistic shaped model comprised of 2/3 muscle was considered. The frequency considered was 3 GHz.

Figure 6 shows the effect of the pinna and model heterogeneity on the heating factor and the coefficient of determination. As seen from Fig. 6, no clear difference was observed between the results for different model heterogeneity, together with the pinna. The heating factor was influenced by 5-9% for the averaging mass from 5 to 15 g where the coefficient of determination peaks.

Next, we present in Fig. 7 the effect of iii) the antenna feeding position relative to the head. We have considered five additional positions, together with the original position. These five positions are located at 10 mm away from the original position. As seen from Fig. 7, the heating factor was influenced by 5-7% for the averaging mass from 5 to 15 g. The coefficient of determination is also influenced marginally. Specifically, the coefficient peaked at the same averaging mass.

4. Discussion

Let us discuss our finding in terms of safety guidelines/standards. We cannot compare our results to the metric in the ICNIRP guidelines, since the averaging region for SAR considered in the present study is cubic shape. According to the IEEE standard (2005), the SAR averaged 10 g is used as the basic restriction for local exposure at frequencies smaller than 3 GHz, while incident power density is used for frequencies larger than 3 GHz. In that standard, it is noted that '*compliance with this standard may be demonstrated by evaluation of either incident power density or local SAR to provide a transition in the frequency range 3 GHz to 6 GHz*'. According to our computation, even in the frequencies from 3 to 6 GHz, the averaged SAR over 10 g was still reasonably correlated with the local temperature elevation, although the correlation became relatively worse as compared with lower frequencies (Bit-Babik 2007, Hirata et al. 2008, Razmadze 2009). Namely, our results could support the above description in the IEEE safety standard. Recently, measurement standard tend to extend the frequency from 3 GHz to 6 GHz. The extension of the upper frequency in the measurement standard would be reasonable from the standpoint of protection for microwave-induced temperature elevation.

5. Summary

The present study investigated the relationship between temperature elevation and

mass-averaged specific absorption rate (SAR) in anatomically-based Japanese head models due to a dipole antenna. The frequency region considered was from 1 to 6 GHz, which includes the frequency where some discrepancy is found in the applicable frequencies between IEEE (2003) and IEC (2005, 2008) for the SAR measurements. Our attention focused on the averaging mass of SAR, which maximizes the correlation with temperature elevation over the head model. Even in the frequencies from 3 to 6 GHz, the averaged SAR over 10 g was still reasonably correlated with the local temperature elevation, although the correlation became relatively worse as compared with lower frequencies (Bit-Babik 2007, Hirata et al. 2008, Razmadze 2009). This tendency was marginally influenced by the effect of the pinna, model inhomogeneity, and the antenna position relative to the head model.

The SAR averaging mass which maximized the correlation was 5-25 g for the homogeneous cubical model. This averaging mass roughly corresponds to a cube with a side length of 15-30 mm. At 6 GHz, the penetration depth of the electromagnetic waves is 4 mm. Conversely, the thermal diffusion length is on the order of a few centimeters or more, depending on the thermal constants of the tissues (Hirata et al. 2007). Based on these facts, the dominant factor influencing the averaging mass of SAR was the heat diffusion length, which depends on the blood perfusion rate of the tissue. The average mass of 1 g was not a good indicator of a temperature increase even with frequencies between 3 and 6 GHz.

The heating factor for the NICT model was 15-20% smaller than that computed for the NIT model. The coefficient of determination for the NICT model peaks at a larger averaging mass than that for the NIT model. Hirata et al. (2006), Samaras et al (2007), and Laakso (2009) investigated the maximum temperature elevation due to RF exposure and found that the tissue composition influenced the correlation between mass-averaged SAR and temperature elevation. Namely, the dominant factor influencing the heating factor and averaging mass is the heat diffusion length. The higher the blood perfusion rate is, the smaller the heating factor and the smaller the SAR averaging mass, which maximizes the correlation with the temperature.

ACKNOWLEDGEMENT

This work was supported in part by the Strategic Information and Communications R&D Promotion Programme (SCOPE).

REFERENCES

Adair E. R., Adams B. W., and Akel G. M. 1984 Minimal changes in hypothalamic temperature

accompanymicrowave-induced alteration of thermoregulatory behavior *Bioelectromagnetics*, **5** 13–30

Bernardi P, Cavagnaro M, Pisa S, and Piuzzi E. 2000 Specific absorption rate and temperature increases in the head of a cellular-phone user *IEEE Trans. Microwave Theory Tech.* **48** 1118–26

Bernardi P, Cavagnaro M, Pisa S, and Piuzzi E. 2003 Specific absorption rate and temperature increases in the head of a cellular-phone user *IEEE Trans. Microwave Theory & Tech.* **48** 1118-26

Bit-Babik G, Faraone A, Chou CK, Radmadze A, Zaridze R. 2007 Correlation between locally averaged SAR distribution and related temperature rise in human body exposed to RF field *Proc. BEMS 2007*, 2-5

Buccella C, De Santis V, Feliziani M. 2007 Prediction of temperature increase in human eyes due to RF sources *IEEE Trans. Electromagnetic Compat*. **49** 825-833

Burkhart M and Kuster N. 2000 Appropriate modeling of the ear for compliance testing of handheld MTE with SAR safety limits at 900/1800 MHz *IEEE Trans. Microwave Theory Tech.* **48** 1927–34

Duck F A. 1990 Physical Properties of Tissue. New York: Academic

Fiala D, Lomas K J, and Stohrer M. 1999 A computer model of human thermoregulation for a wide range of environmental conditions: the passive system *J Appl Physiol.* **87** 1957-72

Flyckt V M M., Raaymakers B W., Kroeze H., Lagendijk J J W. 2007 Calculation of SAR and temperature rise in a high-resolution vascularized model of the human eye and orbit when exposed to a dipole antenna at 900, 1500 and 1800 MHz *Phys. Med. Biol.* **52** 2691-701

Gabriel S, Lau RW, and Gabriel C 1996 The dielectric properties of biological tissues: III. Parametric models for the dielectric spectrum of tissues *Phys. Med. Biol.* **41** 2271-293

Gandhi O. P., Li QX, and Kang G. 2001 Temperature rise for the human head for cellular telephones and for peak SARs prescribed in safety guidelines *IEEE Trans. Microwave Theory Tech.* **49** 1607-1613

Gandhi OP, Lazzi G, and Furse CM, Electromagnetic absorption in the human head and neck for mobile telephones at 835 and 1900 MHz *IEEE Trans Electromagnetic Compat.* **44** 1884-97

Guyton AC and Hall JE. 1996 Textbook of Medical Physiology, Philadelphia, PA: W. B. Saunders

Hardy JD, Wolff HG, and Goodell H. 1952 Pain Sensation and Reactions, Baltimore, MD: Williams & Wilkis

Hirata A, Matsuyama S, and Shiozawa T. 2000 Temperature rises in the human eye exposed to EM waves in the frequency range 0.6-6 GHz *IEEE Trans Electromagnetic Compat*. **42**

386-393

Hirata A, Morita M, and Shiozawa T. 2003a Temperature increase in the human head for dipole antenna at microwave frequencies *IEEE Trans. Electromagnetic Compat.* **45** 109-116.

Hirata A and Shiozawa T. 2003b Correlation of maximum temperature increase and peak SAR in the human head due to handset antennas *IEEE Trans. Microw. Theory Tech.* **51** 1834–1841.

Hirata A, 2005 Temperature increase in human eyes due to near-field and far-field exposures at 900 MHz, 1.5 GHz, and 1.9 GHz *IEEE Trans. Electromagnetic Compat.* **47** 68-76.

Hirata A, Fujimoto M, Asano T, Wang J, Fujiwara O, and Shiozawa T. 2006 Correlation between maximum temperature increase and peak SAR with different average schemes and masses. *IEEE Trans. Electromagnetic Compat*. **48** 569-78

Hirata A, Watanabe S, Fujiwara O, Kojima M, Sasaki K, and Shiozawa T. 2007 Temperature elevation in the eye of Japanese male and female models for plane wave exposure *Phys. Med. Biol.* **52** 6389-99

Hirata A, Shirai K, and Fujiwara O. 2008 On averaging mass of SAR correlating with temperature elevation due to a dipole antenna *Prog. Electromagnetic Res.* **84** 221-237

Ibrahiem A., Dale, C, Tabbara, W, Wiart J. 2005 Analysis of the temperature increase linked to the power induced by RF source *Prog Electromagnetics Res,* **52**, 23-46

ICNIRP 1998 Guidelines for limiting exposure to time-varying electric, magnetic, and electromagnetic fields (up to 300 GHz) *Health Phys.* **74**, 494-522

IEC62209-1. 2005 Human exposure to radio frequency fields from hand-held and body-mounted wireless communication devices -Human models, instrumentation, and procedures- Part 1: Procedure to determine the specific absorption rate (SAR) for hand-held devices used in close proximity to the ear (frequency range of 300 MHz to 3 GHz)

IEC62209-2 Draft. 2008 Human exposure to radio frequency fields from hand-held and body-mounted wireless communication devices -Human models, instrumentation, and procedures- Part 2: Procedure to determine the specific absorption rate (SAR) for wireless communication devices used in close proximity to the human body (frequency range of 30 MHz to 6 GHz)

IEEE C95.3. 2002 Recommended Practice for Measurements and Computations of Radio Frequency New York: IEEE

IEEE P1528. 2003 IEEE Recommended Practice for Determining the Peak Spatial-Average Specific Absorption Rate (SAR) in the Human Head from Wireless Communications Devices: Measurement Techniques.

IEEE C95-1. 2005 IEEE standard for safety levels with respect to human exposure to radio

frequency electromagnetic fields, 3 kHz to 300 GHz,

Laakso I. 2009 Assessment of the computational uncertainty of temperature rise and SAR in the eyes and brain under far-field exposure from 1 to 10 GHz *Phys. Med. Biol.* **54** 333-3404

Neufeld E, Chavannes N, Samaras T and Kuster N. 2007 Novel conformal technique to reduce staircasing artifacts at material boundaries for FDTD modeling of the bioheat equation *Phys. Med. Biol.* **52** 4371-81

Pennes HH. 1948 Analysis of tissue and arterial blood temperature in resting forearm *J Appl Physiol*. **1** 93-122

Razmadze A, Shoshiashvili, L, Kakulia D, Zaridze R, Bit-Babik G, and Faraone A. 2009 Influence of specific absorption rate averaging schemes on correlation between mass-averaged absorption rate and temperature rise *Electromagnetics* **29** 77-90

Samaras T, Christ A and Kuster N. 2006 Effects of geometry discretization aspects on the numerical solution on the bioheat transfer equation with the FDTD technique *Phys. Med. Biol.* **51** N221-9

Samaras T, Kalampaliki, Sahalos JN. 2007 Influence of thermophysiological parameters on the calculations of temperature rise in the head of mobile phone users *IEEE Trans. Electromagnetic Compat.* **49** 936-39

Van Leeuwen GMJ, Lagendijk JJW, Van Leersum BJAM, Zwamborn APM, Hornsleth SN, and Kotte ANTJ. 1999 Calculation of change in brain temperatures due to exposure to a mobile phone *Phys. Med. Biol.* **44** 2367–2379

Wang J and Fujiwara O. 1999 FDTD computation of temperature rise in the human head for portable telephones *IEEE Trans. Microwave Theory Tech.* **47** 1528–1534

Wang J and Fujiwara O. 2002 Dosimetric evaluation of human head for portable telephones *Electron. Commun. Japan*, Part I, **85**, 12–22

Watanabe S, Taki M, Nojima T, Fujiwara O. 1996 Characteristics of the SAR distributions in a head exposed to electromagnetic fields radiated by a hand-held portable radio *IEEE Trans. Electromagnetic Compat.* **44** 1874-83

Figure and Table Caption

Figure 1: Antenna position relative to (a) homogeneous cubical model and (b) anatomically based head model developed at NIT.

Figure 2: Frequency dependency of (a) heating factor and (b) coefficient of determination on SAR averaging mass in homogeneous cubical model.

Figure 3: Dependence of (a) heating factor and (b) coefficient of determination on blood perfusion rate in homogeneous cubical model at 1 GHz. (c) and (d) represent for heating factor and coefficient of determination for 6-GHz exposure.

Figure 4: (a) Heating factor and (b) coefficient of determination in anatomically based head model developed at NIT.

Figure 5: (a) Heating factor and (b) coefficient of determination in anatomically based head model developed at NICT.

Figure 6: Effect of model inhomogeneity and pinna on (a) heating factor and (b) coefficient of determination in anatomically based head model developed at NIT.

Figure 7: Effect of antenna position relative to humans on (a) heating factor and (b) coefficient of determination in anatomically based head model developed at NIT.

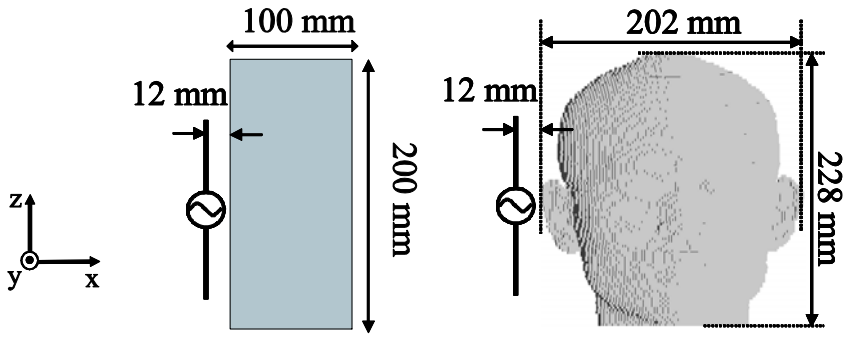

Figure 1

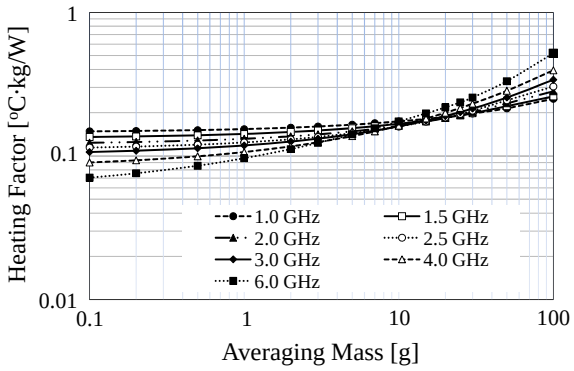
Heating Factor [ºC·kg/W]
1
0.1
0.01
0.1
1
10
100
Averaging Mass [g]
1.0 GHz
1.5 GHz
2.0 GHz
2.5 GHz
3.0 GHz
4.0 GHz
6.0 GHz

(a)

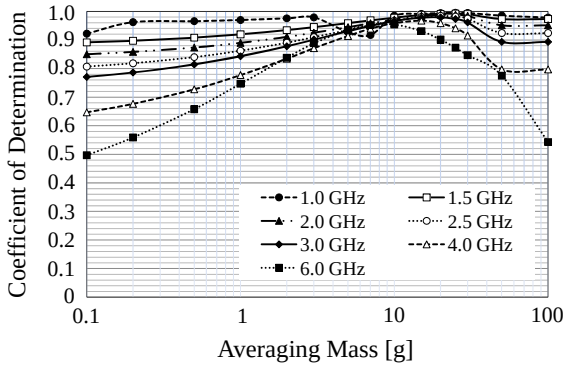
Coefficient of Determination
1.0
0.9
0.8
0.7
0.6
0.5
0.4
0.3
0.2
0.1
0
0.1
1
10
100
Averaging Mass [g]
1.0 GHz
1.5 GHz
2.0 GHz
2.5 GHz
3.0 GHz
4.0 GHz
6.0 GHz

(b)

Figure 2

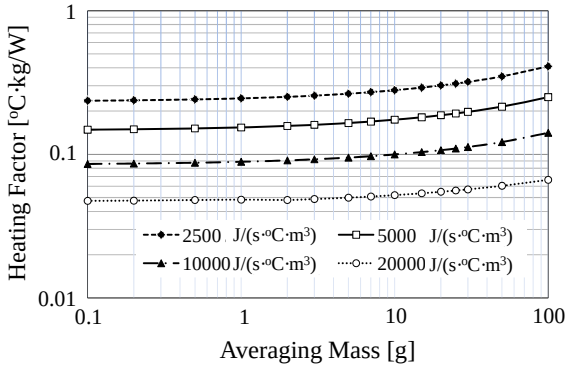
Heating Factor [ºC·kg/W]
1
0.1
0.01
0.1
1
10
100
Averaging Mass [g]
2500 J/(s·ºC·m³)
5000 J/(s·ºC·m³)
10000 J/(s·ºC·m³)
20000 J/(s·ºC·m³)

(a)

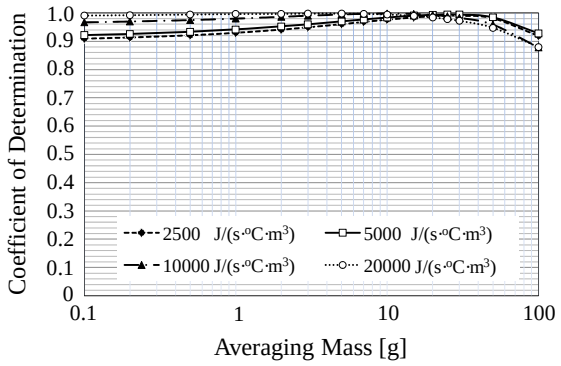
Coefficient of Determination
1.0
0.9
0.8
0.7
0.6
0.5
0.4
0.3
0.2
0.1
0
0.1
1
10
100
Averaging Mass [g]
2500 J/(s·ºC·m³)
5000 J/(s·ºC·m³)
10000 J/(s·ºC·m³)
20000 J/(s·ºC·m³)

(b)

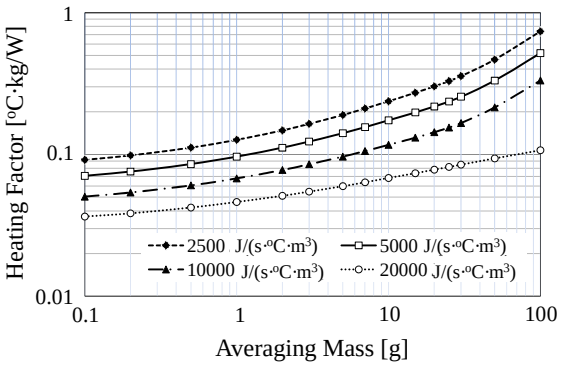
Heating Factor [ºC·kg/W]
1
0.1
0.01
0.1
1
10
100
Averaging Mass [g]
2500 J/(s·ºC·m³)
5000 J/(s·ºC·m³)
10000 J/(s·ºC·m³)
20000 J/(s·ºC·m³)

(c)

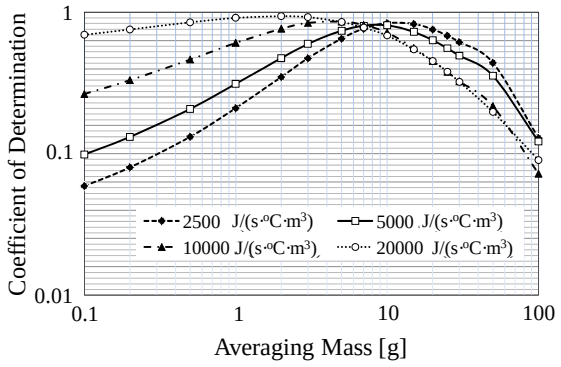
Coefficient of Determination
1
0.1
0.01
0.1
1
10
100
Averaging Mass [g]
2500 J/(s·ºC·m³)
5000 J/(s·ºC·m³)
10000 J/(s·ºC·m³)
20000 J/(s·ºC·m³)

(d)

Figure 3

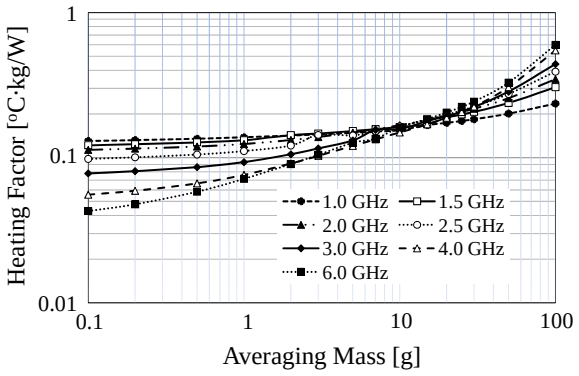
Heating Factor [°C·kg/W]
1
0.1
0.01
0.1
1
10
100
Averaging Mass [g]
1.0 GHz
1.5 GHz
2.0 GHz
2.5 GHz
3.0 GHz
4.0 GHz
6.0 GHz

(a)

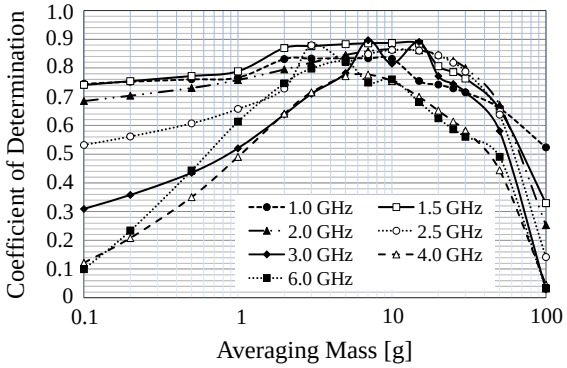
Coefficient of Determination
1.0
0.9
0.8
0.7
0.6
0.5
0.4
0.3
0.2
0.1
0
0.1
1
10
100
Averaging Mass [g]
1.0 GHz
1.5 GHz
2.0 GHz
2.5 GHz
3.0 GHz
4.0 GHz
6.0 GHz

(b)

Figure 4

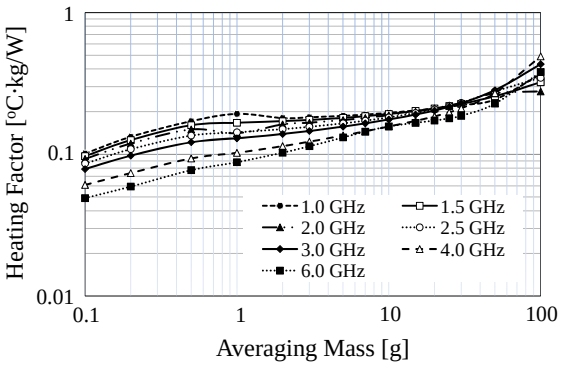
Heating Factor [ºC·kg/W]
1
0.1
0.01
0.1
1
10
100
Averaging Mass [g]
1.0 GHz
1.5 GHz
2.0 GHz
2.5 GHz
3.0 GHz
4.0 GHz
6.0 GHz

(a)

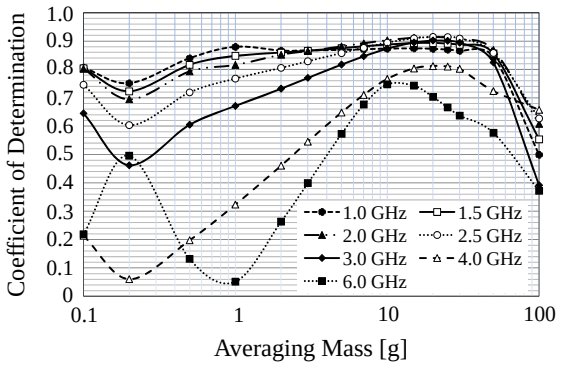
Coefficient of Determination
1.0
0.9
0.8
0.7
0.6
0.5
0.4
0.3
0.2
0.1
0
0.1
1
10
100
Averaging Mass [g]
1.0 GHz
1.5 GHz
2.0 GHz
2.5 GHz
3.0 GHz
4.0 GHz
6.0 GHz

(b)

Figure 5

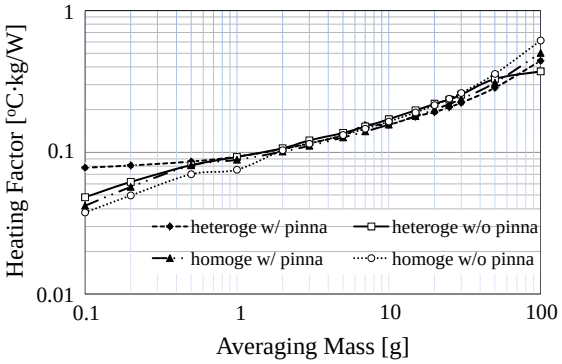
Heating Factor [ºC·kg/W]
1
0.1
0.01
0.1
1
10
100
Averaging Mass [g]
heteroge w/ pinna
heteroge w/o pinna
homoge w/ pinna
homoge w/o pinna

(a)

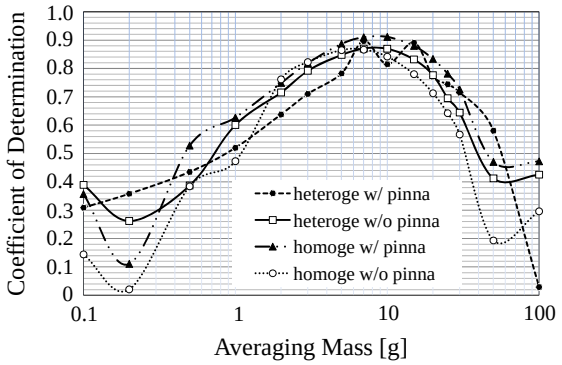
Coefficient of Determination
1.0
0.9
0.8
0.7
0.6
0.5
0.4
0.3
0.2
0.1
0
0.1
1
10
100
Averaging Mass [g]
heteroge w/ pinna
heteroge w/o pinna
homoge w/ pinna
homoge w/o pinna

(b)

Figure 6

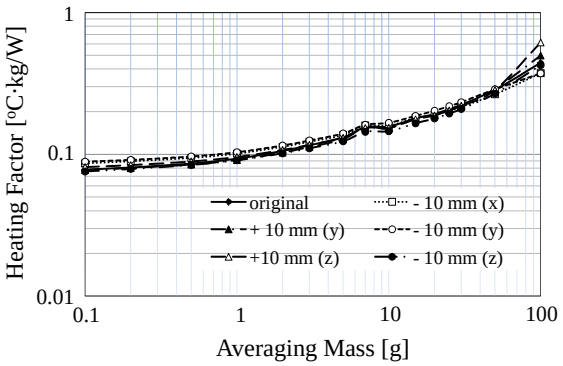
Heating Factor [ºC·kg/W]
1
0.1
0.01
0.1
1
10
100
Averaging Mass [g]
original
- 10 mm (x)
+ 10 mm (y)
- 10 mm (y)
+10 mm (z)
- 10 mm (z)

(a)

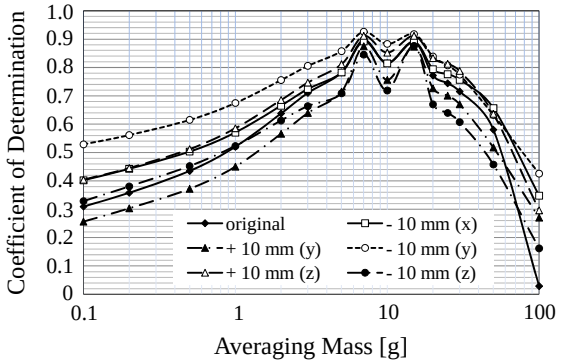
Coefficient of Determination
1.0
0.9
0.8
0.7
0.6
0.5
0.4
0.3
0.2
0.1
0
0.1
1
10
100
Averaging Mass [g]
original
- 10 mm (x)
+ 10 mm (y)
- 10 mm (y)
+ 10 mm (z)
- 10 mm (z)

(b)

Figure 7